Image invariance with changes in size: the role of peripheral contrast thresholds

Eli Peli

Physiological Optics Unit, Eye Research Institute, 20 Staniford Street, Boston, Massachusetts 02114

Jian Yang

Department of Psychology, Northeastern University, Boston, Massachusetts 02115

Robert B. Goldstein

Eye Research Institute, 20 Staniford Street, Boston, Massachusetts 02114

Received October 2, 1990; revised manuscript received June 10, 1991; accepted June 12, 1991

The appearance of objects generally does not change with changes in the size of their retinal image that occur as the distance from the observer increases or decreases. Contrast constancy ensures this invariance for suprathreshold image features, but fully robust size invariance also requires invariance at threshold, so that near-threshold image features do not appear or disappear with distance changes. Since the angular size and the eccentricity of image features covary with distance changes, the threshold requirement for invariance could be satisfied approximately if contrast thresholds were to vary as the product of the spatial frequency and the eccentricity from the fovea. This model fits contrast thresholds for orientation identification over spatial frequencies of 1–16 cycles/deg and for retinal eccentricities of as much as 23 deg. Contrast detection thresholds from six different studies conform to this model over an even wider range of spatial frequencies and retinal eccentricities. The fitting variable, the fundamental eccentricity constant, was similar for all three studies that measured detection along the horizontal meridian and was higher for the orientation identification contrast thresholds along the same meridian. The eccentricity constant from studies that measured detection along the vertical meridian was higher than the constant calculated for the horizontal meridian and lower than the eccentricity constant for chromatic isoluminance gratings. Our model and these results provide new tools for analyzing the visibility of displays and for designing equal-visibility or variable-visibility displays.

INTRODUCTION

It is frequently stated that the visual system is constructed and operates in a way that is invariant to object changes relative to the observer. Sutherland[1] listed size invariance as the first condition to be fulfilled by a satisfactory theory of visual pattern recognition in animals and humans. He cited studies showing that many species can classify a shape as the same shape regardless of its changes in size, at least over a considerable range, and that this capacity is innate. The spatial frequency spectra of images frequently are defined in terms of cycles per picture width rather than cycles per degree.[2,3] This is done under the assertion that "form perception is largely independent of distance,"[3] which is frequently, though not always, true. Such distance invariance was reported for identification of bandpass-filtered letters embedded in Gaussian noise,[4] for recognition of bandpass-filtered images of faces,[5] and for identification of images of toy tanks.[6] In addition to the invariant appearance of suprathreshold features, invariant perception also requires that important image features remain visible (do not cross the threshold) despite the change in their retinal spatial frequencies associated with the change in distance. In this paper we propose that a property of the visual system causes its detection of image contrast to be nearly invariant to changes in size caused by distance changes. We show that the threshold invariance at various retinal eccentricities is as good as the invariance at the fovea. For spatial frequencies that straddle the peak of the contrast sensitivity function (CSF) the deviation from optimal invariance is small.

Invariance of Suprathreshold Contrast

A system that has size invariance must meet several constraints. When the distance between an object and an observer changes, the spatial frequency content of its retinal image changes. Since the sensitivity of the visual system is highly dependent on spatial frequency, changes in the appearance of the image of the object could be anticipated, but they are not observed. Georgeson and Sullivan[7] discussed this effect and suggested an explanation for the invariant appearance of suprathreshold features of images under such distance changes. The visual system response to suprathreshold stimuli varies as a function of spatial frequency differently than does the threshold response.[8] In contrast-matching experiments subjects adjusted the apparent contrast of a variable frequency test grating to match the contrast of the standard grating at 5 cycles/deg.[7] When the standard grating was presented at a low, near-threshold contrast, the contrast of the comparison grating at other frequencies was set at a higher value. The relation could be predicted from the CSF.

0740-3232/91/111762-13$05.00 © 1991 Optical Society of America

Above threshold a test grating of one frequency was adjusted to the same physical contrast as a standard of another frequency despite large differences in sensitivities to the frequencies.[7] This result is surprising, because the optical effects of the media produce substantially different retinal contrasts for the two gratings. Thus at suprathreshold contrast levels the visual system compensates for the blurring effects of the eye's optics. This behavior was termed contrast constancy and is important for image invariance with distance, since it ensures that suprathreshold features of high-contrast images will remain invariant despite the effect of the eye's optics.

Georgeson and Sullivan[7] proposed a simple model based on multiple spatial frequency channels that have variable gains with higher gains for high spatial frequencies. The results of experiments with amblyops suggest that this compensation occurs at the level of the visual cortex.[7,9] Stephens and Banks[10] demonstrated that this effect of contrast constancy can be observed in infants aged 12 weeks and older but is absent in 6-week-old infants. They further discussed various possible mechanisms that the visual system may use to recalibrate its suprathreshold gain at different spatial frequencies.

At suprathreshold levels distance invariance is achieved, as the visual system does satisfy the requirement for linear scale invariance.[11] However, the requirements are attained at the limiting, trivial case of a standard Fourier transform. The requirements for complete scale invariance for linear systems, as set forth by Klopfenstein and Carlson,[12] are quite strict. They demand that a change in size will not change the functional form of the resultant image or its Fourier transform at all. In fact the visual system can easily identify shapes of objects whose spectra are slightly or even significantly changed (i.e., high-pass–filtered images). The theory of shape-invariant linear imaging systems[12] cannot be applied directly to threshold-level images.

Invariance of Contrast at Threshold

The effect of contrast constancy[7,8] ensures invariance with distance changes only for image features whose contrast is substantially above threshold. Lower-contrast features are affected by distance changes unless compensated for by another mechanism. Such compensation is important, since distance-induced changes of image features across the threshold, from visible to invisible, would affect the perception of images more than the variations in contrast at suprathreshold levels. Image features usually do not appear or disappear with distance changes. The simplest way to achieve distance invariance would be to have equal contrast thresholds at all spatial frequencies and retinal eccentricities. This is not the case; the CSF does vary with the spatial frequency and the eccentricity. However, a less stringent constraint can be realized, owing to the covariance of the angular size and the eccentricity of image features with distance changes. When an object moves farther from the observer, the spatial frequency of various features in the object increases. At the same time, the overall size of the object's retinal image decreases. Therefore many of these features now can fall on retinal areas closer to the fovea, where contrast sensitivity is higher. Thus, at threshold, the requirements for invariance could be satisfied if contrast thresholds were to vary as the product of the spatial frequency and the retinal eccentricity:

$$T(\theta, f) = G(\theta f), \tag{1}$$

where θ is the retinal eccentricity and f is the spatial frequency. For example, if an object doubles its distance from the observer, its spatial frequency content is shifted to double the frequency, but the distance of features from the fovea is halved. Features that are suprathreshold remain visible, and those that are subthreshold remain undetectable with the distance change, if the contrast sensitivity at the doubled frequency at this new retinal location is the same.

Measured contrast thresholds at any one spatial frequency increase exponentially with the eccentricity, as is shown below. Thus on a logarithmic scale the threshold varies linearly with the eccentricity. If we want features that are visible to stay visible and those that are invisible to stay invisible with distance changes, then the threshold at all spatial frequencies should be related to the eccentricity in a specific way (Fig. 1). The required condition is

$$T(\theta, f) = A \exp(a\theta f), \tag{2}$$

where T is the contrast threshold and a is a constant.

With this model the threshold at the fovea ($\theta = 0$) stays the same (i.e., A) for all spatial frequencies. We know that this is not the case, since foveal thresholds vary with spatial frequency. Indeed, when an object is moved to a great distance invariance breaks down; the object becomes blurred, then indistinguishable, and eventually disappears.

However, for a large range of distances invariance may be possible with regard to the normalized threshold, T_r; the normalized threshold (i.e., threshold/foveal threshold) is the distal contrast threshold normalized by the foveal distal threshold. Distal contrast is the contrast measured at the object. (Distal contrast is distinguished here from retinal contrast.) Thus invariance of the normal-

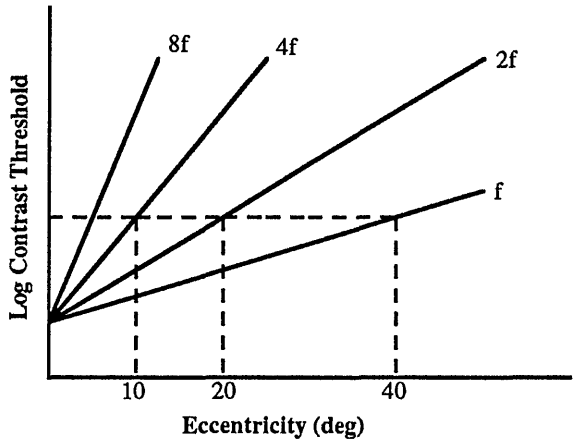

Fig. 1. Hypothetical contrast threshold as a function of eccentricity for various spatial frequencies that would maintain invariant image perception with distance. The slopes of the lines have the same ratios as the corresponding spatial frequencies. If a threshold feature at spatial frequency $2f$ and an eccentricity of 20 deg is shifted by the change of distance to spatial frequency $4f$ but at the same time approaches an eccentricity of 10 deg from the fovea, then it will remain at the threshold level despite these changes.

ized threshold is achieved if the peripheral threshold is varied as

$$T_r(\theta, f) = \frac{T(\theta, f)}{T(0, f)} = \exp(a\theta f), \quad (3)$$

where $T(0, f)$ is the threshold for spatial frequency f at the fovea. Similar normalization was used by Fleck[13] for comparison of target detection and discrimination at different eccentricities and by Mullen[14] for comparison of luminance contrast sensitivity with color contrast sensitivity.

With this suboptimal invariance features at any eccentricity will cross the distal threshold with distance changes under the same conditions that will cause such a crossing in the fovea. For high spatial frequencies this limitation may be severe; for example, a 5 cycles/deg suprathreshold feature[15] at any eccentricity will remain visible under a fourfold increase in distance only if its initial contrast was at least 10 times the threshold contrast, the same contrast-to-threshold ratio that is required for a foveal grating pattern to remain visible as it shrinks from 5 to 20 cycles/deg.[16] The deviation from invariance is smaller for moderate frequencies that straddle the peak of the CSF. For example, a threshold-level feature of 2 cycles/deg will remain at threshold under a similar fourfold increase in distance, since the foveal thresholds for 2 and 8 cycles/deg are almost equal.

In this paper we test the conformity of contrast threshold data to this model for both contrast detection thresholds and contrast thresholds for orientation identification. Since there are numerous studies of contrast detection,[17–20] we fitted the model to existing published data. There is no such body of data for orientation identification contrast threshold in the periphery. Although foveal detection thresholds show the same dependence on spatial frequency as do contrast thresholds for discrimination between horizontal to vertical gratings,[21,22] form discrimination generally falls faster with eccentricity than does detection.[13,23]

METHODS

Contrast Thresholds for Orientation Identification

The threshold contrast required for discrimination between horizontal and vertical sinusoidal grating patches (Gabor functions) was measured for two subjects. Measurements were taken at the fovea and at temporal eccentricities of 2.5, 5.1, 10.3, and 22.8 deg in the right eye. Thresholds at each eccentricity were measured for five spatial frequencies, 1, 2, 4, 8, and 16 cycles/deg. Stimuli were generated with an Adage 3000 image processor with a 10-bit digital-to-analog converter and were displayed on a US Pixel (PX 19) 60-Hz noninterlaced monochrome monitor.

The Gabor-function stimuli were composed of either horizontal or vertical sinusoidal gratings in cosine phase multiplied by a two-dimensional Gaussian envelope. For the vertical gratings of frequency f_0 the patch can be described as

$$p(x, y) = L_0\left[1 + m\cos(2\pi f_0 x)\exp\left(-\frac{x^2 + y^2}{\sigma^2}\right)\right], \quad (4)$$

where L_0 is the mean luminance, m is the nominal contrast, and σ is the spatial spread of the Gaussian envelope. For the 1-octave patches used, $\sigma = 3P/\pi$, where $P = 1/f_0$ is the period of the sinusoidal grating in degrees.

Our stimuli contained $12/\pi$ cycles (~4); however, only approximately two cycles were visible because of the rapid decline of the envelope. The surrounding screen luminance was matched with a mean luminance of 37.5 cd/m^2 for all presentations. The video display spanned 8 deg × 8 deg at the observation distance of 203 cm (80 in.). There was additional surrounding screen, matched with luminance and color to the video screen, that extended 30 deg from the center of the video screen on the right and 10 deg from the center of the video screen to the left. A fixation point was generated on the video screen for an eccentricity of 2.5 deg, and LED targets were used for fixation at the greater eccentricities. The subject maintained fixation at one eccentricity for each session, and the lower four spatial frequencies were interleaved during the session. Measurements of the 16-cycles/deg stimuli were taken at 381 cm (150 in.) from the screen and were interleaved with 8-cycle/deg stimuli. Only the data for 16 cycles/deg at that distance were analyzed.

Stimuli were presented in a two-alternative, forced-choice paradigm. The pattern was presented for 0.5 s with an abrupt onset and offset. The subject pressed a button to present a grating patch. The subject then indicated whether the grating patch was horizontal or vertical and received auditory feedback. The psychophysical procedure was a hybrid method, consisting of three successive procedures.[24] The sequence started with a staircase procedure that ran to the second reversal of direction. The procedure then changed to a modified parameter-estimation-by-sequential-testing (PEST) method.[25] In the second phase stimulus contrast was controlled by the staircase, but the data were collected and analyzed by the PEST algorithm. When the PEST routine found an initial threshold estimate (five-step confidence level of more than 40%), stimulus contrast control was switched to the PEST. With this method 50–80 presentations were necessary to reach the termination criteria (three-step confidence level of 50%). Contrast was changed in 0.1-log-unit steps. After termination a Weibull psychometric function was fitted to the data to yield a threshold estimate. The slope of the psychometric function was not fixed and was fitted as well. The analysis also provided a sampling of statistics for the threshold, $\hat{se}$, that is comparable with the standard error of the mean.

Contrast Detection Thresholds from Previous Studies

In addition to analyzing our orientation discrimination threshold data, we tested the conformity to the same model of contrast detection threshold data that were obtained in other independent studies.[14,17–20] The various studies covered different but overlapping spatial frequency and eccentricity ranges. Different spatial and temporal windows stimuli and different psychophysical paradigms were used for testing along different meridia. Cannon[19] used 2-deg-diameter vertical sine-wave grating patches. Thresholds were measured by the method of limits with six trials, three with increasing contrast and three with decreasing contrast. Stimuli were presented to the right of fixation for 2 s, including 350-ms rise and

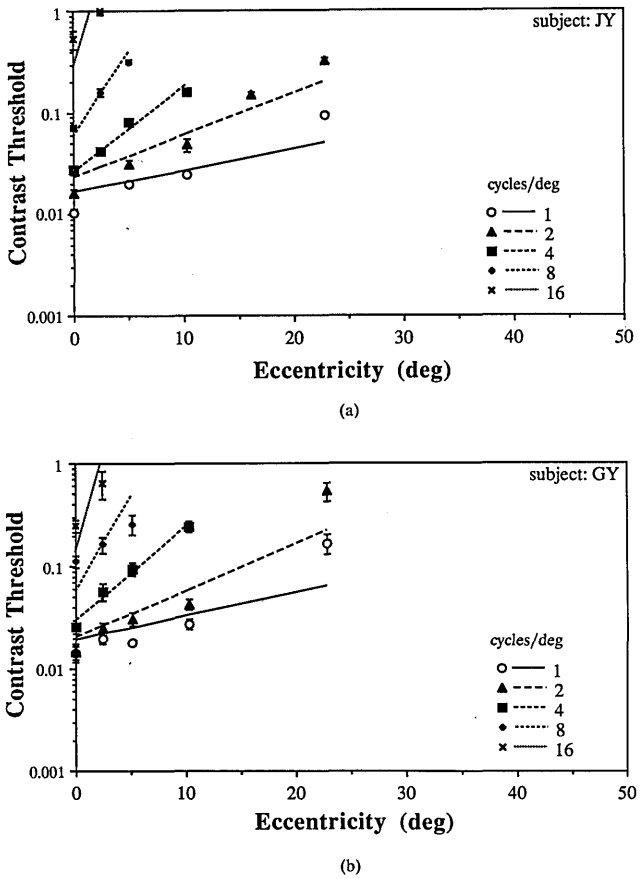

Fig. 2. Contrast thresholds for orientation identification of two observers at different spatial frequencies, measured as a function of eccentricity. Lines represent the fit of the model to the data. All five lines were fitted together, and the slopes of the lines were constrained to have the same ratios as the corresponding spatial frequencies (factors of 2, in this case). The eccentricity constant a, representing the slope at 1 cycle/deg, is 0.048 and 0.053 for subjects JY and GY, respectively. Error bars represent the estimate of the standard error of the mean, $\hat{se}$.

fall times. Pointer and Hess[17] presented horizontally oriented sinusoidal grating patches in Gaussian envelopes. The spatial frequency bandwidth was 0.24 octave (6.4 periods). A temporal, two-alternative, forced-choice technique with feedback measured monocular contrast detection thresholds. A Gaussian window with a short temporal spread (width at 1/*e* of maximum) of 250 ms was used to reduce the effects of eye movements. We analyzed data for one subject along the horizontal meridian (Fig. 3A of Ref. 17). Robson and Graham[18] used 4-cycle patches of horizontal grating presented along the vertical meridian in a Gaussian temporal window with a temporal spread of 100 ms. A two-temporal-alternatives forced-choice staircase was used to determine the 90% correct responses threshold. Thomas[20] used a circular patch, 3 deg in diameter presented for 1 s, either with an abrupt onset and offset or ramped on and off over the whole second. Targets were presented to the superior retina by using a two-by-two procedure, combining a two-alternative temporal forced-choice detection task with a two-alternative identification task. Mullen[14] measured the detection threshold for chromatic isoluminance gratings. A sharp-edged circular patch of 4 cycles, sinusoidally phase reversed at 0.4 Hz, was presented along the horizontal

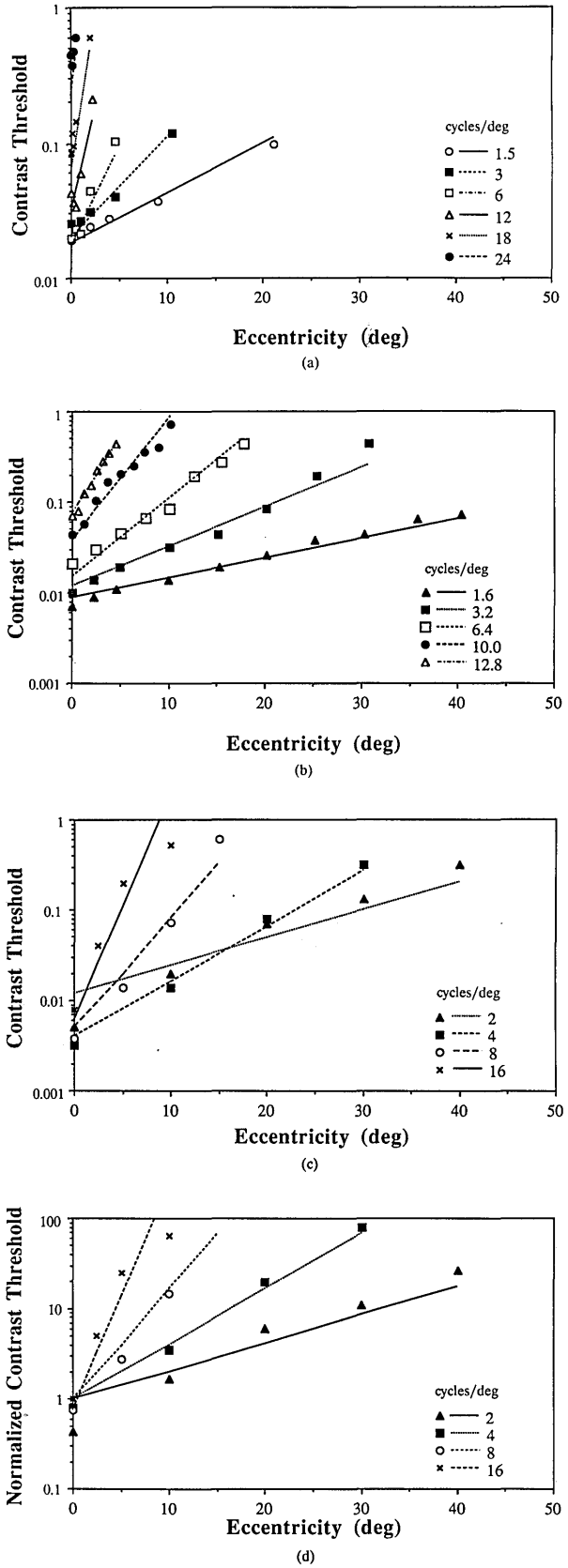

Fig. 3. Contrast detection threshold data (symbols) as a function of eccentricity together with the fit of our model (lines) to data from three different studies: (a) data from Ref. 18, (b) data from Ref. 17, (c) data from Ref. 19. (d) The same data and fits as in (c), displayed as normalized thresholds, i.e., threshold divided by (calculated) foveal thresholds. The normalized graph makes it easier to appreciate visually the closeness of the fit of our model to these data.

meridian. The ascending method of adjustment was used to determine the threshold from four separate settings.

Fitting the Model to the Data

The log contrast threshold data were plotted as a function of retinal eccentricity with spatial frequency as the parameter. The data for each spatial frequency on a log scale could be well fitted with a straight line (see below). To test the agreement with the model, the data for all spatial frequencies and eccentricities were fitted simultaneously with a constrained set of straight lines. The slopes of the lines were constrained to have the same ratio as the corresponding spatial frequencies. The whole set of data was fitted with

$$\ln[T(\theta, f)] = a\theta f + b(f), \tag{5}$$

where $b(f)$, the zero intercept, represents the natural logarithm of the foveal threshold at frequency f. We calculated the set of variables that provided the minimum mean-square-error fit by using the general linear model (PROC GLM) procedure in the SAS software system for data analysis (SAS Institute, Cary, N.C.). The mean-square-error fit of these sets of lines was obtained by determining $b(f)$ simultaneously for all frequencies tested and finding a single value for the parameter a. The parameter a obtained in this way can be interpreted as the slope of the line associated with spatial frequency of 1 cycle/deg, and thus we call it the fundamental eccentricity constant.

RESULTS

Contrast Thresholds for Orientation Identification

Figure 2 shows the contrast thresholds for orientation for the two subjects at various spatial frequencies and eccentricities. The lines represent the simultaneous fits of the model for spatial frequencies 1, 2, 4, 8, and 16 cycles/deg. The values of the eccentricity constant a are close for the two subjects, 0.048 and 0.053 for JY and GY, respectively.

To evaluate the quality of the fit, we compared the portion of the variance accounted for by the calculated fit of our model (coefficient of variance, r^2) with the r^2 obtained by using a less constrained fit in which straight lines were fitted separately for each spatial frequency. The more constrained fit had only six free parameters, compared with the ten parameters for the case in which separate lines are fitted for each of the five frequencies. The less constrained fit resulted in an excellent fit. The portion of variance accounted for by this fit was 0.99 and 0.98 for JY and GY, respectively. Adding the severe constraint of our model that required the covariations of the slopes of the lines reduced r^2 only slightly, to 0.92 and 0.87, respectively.

Contrast Detection Thresholds from Previous Studies

A similar analysis was applied to the contrast detection threshold data from four published studies (a fifth study is discussed below). As a result of the differences in stimuli and paradigms in the different studies, the absolute values of contrast detection thresholds varied substantially among these studies (Fig. 3). For example, the foveal thresholds obtained by Cannon[19] were almost 1 log unit lower than those obtained by Pointer and Hess[17] and by Robson and Graham.[18] In addition, the amount of crossing of the various lines was quite different and in this presentation is the result of the shift of the peak of the CSF at different eccentricities. As a result of such shifts the relative order of sensitivities as a function of spatial frequencies switches at different eccentricities.

Despite these differences, data from the five studies were fitted well by the model proposed above. Here, too,

Table 1. Fundamental Eccentricity Constant a, Calculated for the Data from Various Studies[a]

Contrast Threshold Tasks	a	r^2	
		Separate Fit for Each Frequency	Our Model: All Frequencies Fitted Together
Contrast detection			
Horizontal meridian			
Cannon[19]	0.035	0.97	0.92
Pointer and Hess[17]	0.030	0.99	0.98
Hilz and Cavonius[26]	0.036	0.97	0.96
Vertical meridian			
Robson and Graham[18]			
Upper field	0.057	0.98	0.97
Lower field	0.046	0.99	0.97
Thomas,[20] superior retina			
Subject JT	0.043	0.99	0.95
Subject RT	0.051	0.97	0.90
Subject KS	0.051	0.99	0.98
Equiluminance color gratings			
Mullen[14]			
Nasal field	0.070	0.96	0.95
Temporal field	0.120	0.99	0.99
Orientation identification			
This study, nasal field			
Subject JY	0.048	0.99	0.92
Subject GY	0.053	0.98	0.87

[a] The constants found across studies are highly consistent with considerations of the meridian tested and the task performed. The goodness of the fit was evaluated by comparing the coefficients of variance, r^2, calculated for all studies. r^2 was calculated for the fit of a separate line for each frequency and for the fit of our model with the slopes of the lines constrained to have the same ratio as the corresponding spatial frequencies.

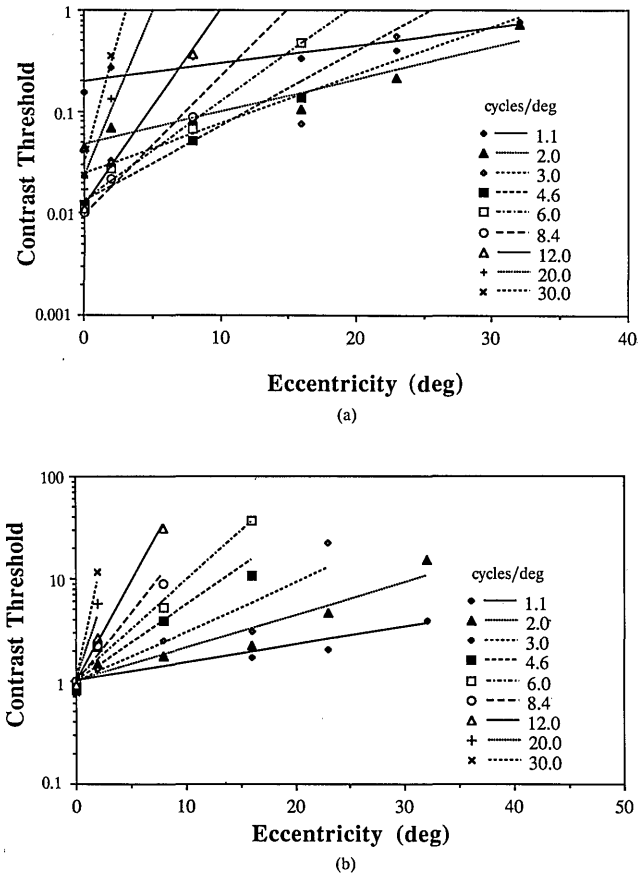

Fig. 4. (a) Retinal contrast detection thresholds as a function of eccentricity, measured with a laser interferometric technique by Hilz and Cavonius.[26] The lines represent the fit of our model to their data. The crossing of the lines here, compared with distal contrast threshold measurements (Fig. 3), represents the effect of neural compensation for the optical degradation of the image. (b) The same data and fits as in (a), displayed in terms of normalized thresholds. This should have been the result of such retinal contrast threshold measurements without neural compensation for the optical modulation transfer function.

the coefficient of variance r^2, obtained with a separate line fit for each spatial frequency, was only slightly better than the r^2 obtained with the fit of our more constrained model (Table 1).

The calculated eccentricity constant, required for the fit of the data from the various studies, was consistent with the differences in the nature of the task (Table 1). The constants calculated for all three studies that measured detection threshold across the horizontal meridian[17,19,26] were similar, 0.035, 0.030, and 0.036, respectively. For the two studies that measured detection threshold along the vertical meridian[18,20] the calculated constants were higher (Table 1). This is in agreement with previous studies that demonstrated a steeper drop in sensitivity along the vertical meridian than the horizontal meridian.[27-29] The eccentricity constant calculated for the data on chromatic isoluminance gratings[14] was even higher, indicating a steeper drop in sensitivity for such gratings than for luminance gratings.

NEURAL COMPENSATION FOR OPTICAL DEGRADATION

The drop in foveal contrast sensitivity as a function of spatial frequencies (for moderate to high frequencies) frequently is assumed to be a result of optical filtering by the eye's media.[30] This assumption arises from the fact that the slope of the CSF is similar to that of the modulation transfer function of the eye's optics. The eye's optics actually account only in part for the slope of the CSF.[16] In fact, quantal fluctuations and other preneural effects all tend to increase the detection threshold as a function of the spatial frequency at any eccentricity. Quantal fluctuations in the stimuli alone account for a slope of -1 in log–log plots for gratings of a fixed number of cycles.[16] If contrast detection thresholds were indeed limited only by the optical modulation transfer function of the eye, then the retinal contrast detection threshold for various spatial frequencies at the fovea (measured with an interferometric technique) should coincide as the normalized contrast thresholds do [e.g., see Figs. 1 and 3(c)]. Such behavior would indicate that the system does not compensate for the effects of the optics at threshold as it does at suprathreshold levels.[7,8] The neural visual system may be capable of compensating, at least partially, for the effects of the optics at threshold. Therefore such compensation would tend to improve the invariant described here. If such compensation takes place, one would expect retinal contrast sensitivity to increase with frequency, as is the case for suprathreshold retinal contrast matching.[31]

Hilz and Cavonius[26] measured retinal contrast sensitivity at various spatial frequencies and eccentricities by using laser interferometry. They used a 2.45-deg field of vertical interference gratings generated with a red He–Ne laser on the observers' retina. The thresholds were determined by the method of adjustment (ascending contrast). Measurements were made with the temporal retina. Their results (their Fig. 3), redrawn in our format (Fig. 4), clearly show the effect of compensation for the optical effects. The fitting of our model to their data is just as good as in the other studies (Fig. 4 and Table 1). The eccentricity contrast calculated for their data (a = 0.036) is in good agreement with the results of two other contrast detection studies. Comparison of the results of all three contrast detection studies demonstrates that some (substantial but less than complete) compensation for the contrast reduction by the eye's optics occurs at threshold as well. Kulikowski[8] also argued that the contrast constancy at suprathreshold levels is incomplete (effective). In Ref. 8, however, the normalization required subtraction of foveal threshold level rather than the division required in our case.

The importance of this apparent neural compensation in the context of our discussion is that it improves the invariance of contrast at threshold. In Eq. (3), the compensation is equivalent to reducing, but not eliminating, the variable (ac) portion of $T(0, f)$. Another interpretation is that, since we have shown that the invariance is equal at all eccentricities, a flat foveal CSF (as a function of spatial frequency) would improve the invariance described here. The bandpass-filtering characteristics of the foveal CSF can be an approximation of a flat CSF over an intermediate range of frequencies. Thus the neural attenuation at low frequencies can be construed as a mechanism for partial compensation for the optical media contrast reduction in an effort to improve the threshold invariance over a range of spatial frequencies centered at the peak frequency of the CSF (4–5 cycles/deg). We recently showed[24] that the relative reduction of sensitivity

(a)

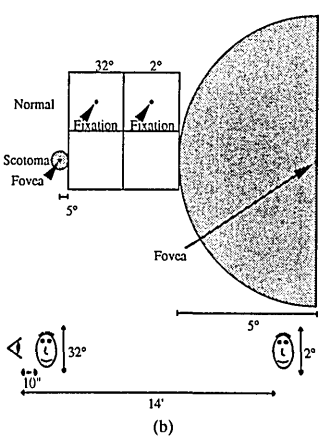

(b)

Fig. 5. (a) Changes in the appearance of a face with a large change in observation distance are illustrated for a normal observer (top) and for a patient with 10-deg-diameter central scotoma (bottom). Images at the left represent the appearance of the face at 25 cm (10 in.) from the observer, where it spans 32 deg of visual angle. Images at the right represent the appearance of the same face 4.3 m (14 ft) from the observer, where it spans only 2 deg of visual angle. The normal observer is assumed to fixate at the center of the face in both cases. The patient is assumed to place the edge of his or her scotoma at the edge of the image in both cases. The changes in appearance for the normal observer are small, limited to the high spatial frequencies and compatible with the filtration of the image by the eye's optical media. The effect of change in distance is much more detrimental for the patient with a central scotoma. At close range the appearance of the face to the patient is almost identical to its appearance to the normal observer. (b) A schematic diagram of the image in (a) and the relation of scotoma and foveal positions to the various images.

at low frequency is actually the result of increased sensitivity at midfrequencies, both for decreased spatial bandwidths and for decreased temporal bandwidths of the stimuli. Further, with 1-octave-wide stimuli, which we suggest are more relevant for form perception,[24] the foveal CSF shape was found to be low pass in character. The flat shape of the function over the low-to-moderate frequencies thus permits almost complete invariance.

SIMULATIONS

The functions obtained through curve fitting can be used to simulate the appearance of images while incorporating the nonuniformity of the visual system. The application of linear image processing to the simulation of the appearance of images to observers[32] has been criticized as involving a double-pass effect.[33] The double-pass effect occurs when the simulated image is presented to the observer through a visual system that is the basis for the simulation. However, with the proper design and within the context of a nonlinear threshold visual system model, it is possible to present valid simulations in which the important details are relatively unaffected by the characteristics of the reader's visual system. Both the processing and the interpretation of the simulation are done in the nonlinear contrast domain rather than in the linear am-

Fig. 6. Simulations presented in Fig. 5 are illustrated here for the cable-car scene that contains more relevant high-frequency information. Both the image invariance for the normal observer and the degradation of the image for the low-vision patient are more dramatic in this case.

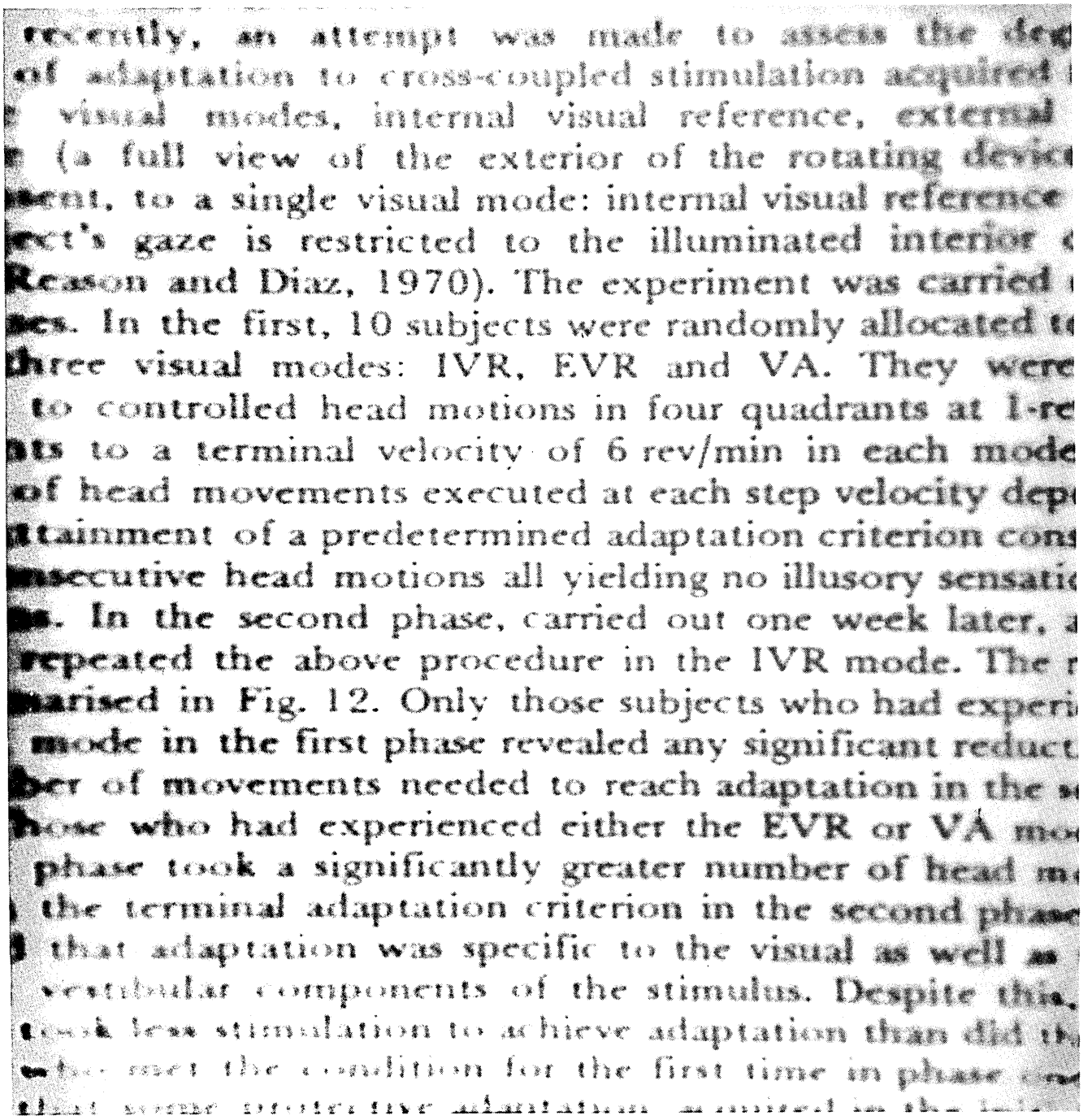

Fig. 7. Simulation of the appearance of newspaper-sized text at a normal reading distance of 25 cm. The section of text illustrated is assumed to span 16 deg of visual angle at a normal reading distance. Fixation is held at the center of the image, and the processing is identical to the one used for Figs. 4 and 5. In this higher-resolution image, it is possible to appreciate the nonuniform aspect of the simulation, which is difficult to note in the previous figures. However, the degradation of image visibility with eccentricity illustrated here is much smaller than the degradation simulated by Yeshurun and Schwartz.[36]

plitude domain. We wish to portray the loss of detail that occurs in viewing objects at a specified distance. We then magnify the image (or, equivalently, examine it from a short distance) so that the surviving fine details are large enough to be seen without being appreciably affected by the reader's visual system. Since the subthreshold information was removed completely, it cannot be altered by the reader's visual system.

We previously presented the method for using contrast threshold data for simulating images with the local band-limited contrast pyramidal structure.[34] In short, the image is sectioned into a series of bandpass filtered versions (of 1-octave bandwidth). For each section we calculated the corresponding local band-limited contrast for each point in the image (by dividing amplitude by the local luminance mean). We then assigned a fixation locus, and for each point in the image the distance from this fixation point was determined. Based on that distance, in degrees, and the spatial frequency associated with the bandpass-filtered version, each point can be tested against

the appropriate threshold to determine whether it will be visible. A suprathreshold point is left unchanged, while a subthreshold point is set to zero contrast. The appearance of the same image from two different distances is obtained by applying the same method of simulation while assigning a different angular span to the image, depending on the observation distance.

The simulations presented here were obtained using the fit of the data of Cannon.[19] Thresholds 1 log unit higher than those measured by Cannon were used. Compared with Cannon's thresholds, these elevated values are in better agreement with the values measured by Pointer and Hess,[17] Robson and Graham,[18] and Hilz and Cavonius.[26] Simulations with one of the other data sets did not differ noticeably from the simulations presented here. Using the low thresholds measured by Cannon resulted in little effect on the processed images. Most of the contrast in the images processed this way was found to be suprathreshold and was not altered. The simulated appearance of a face to a normal observer from a distance of 25 cm (10 in.) is compared in Fig. 5(a) (top row) with the appearance of the same face from 4.3 m (14 ft). In both cases fixation is assumed to be at the center of the image. In both cases there is little apparent change in image quality at different eccentricities. Furthermore, the two images appear to be similar despite the large differences in observation distances. The only noticeable effect is a slight blurring of the fine details for the farther image. Such effects are associated with the suboptimality of the invariance and are included in our simulation. This constancy breaks down for a low-vision observer with a central visual loss of a 5-deg radius, as illustrated in Fig. 5(a) (bottom row). Here we assumed that the observer places the image of the face on his or her retina adjacent to the scotomatous area, i.e., on the most centrally available functional retina.[35] At 25 cm the face appears almost the same to the low-vision observer as it would to the normal observer. However, at 4.3 m, when the face spans only 2 deg of visual angle, the low-vision observer suffers substantial detail loss, and the invariant appearance of the image cannot be maintained. Thus the same mechanism that serves to maintain the appearance of the image for normal observers across this 16-to-1 change in distance results in image deterioration for the patient with central scotoma. The effect is even more dramatic for images that contain more high spatial frequencies than the face's image (Fig. 6). Although the exact images are difficult to reproduce in print, the relationships among the various versions of the simulation are similar to those observed on a calibrated display.

Figure 7 shows the appearance of a small segment of printed text, spanning 16 deg of visual angle and fixated at the center. This image represents the appearance of newspaper-size text at a normal reading distance. Most of the area displayed (16 deg × 16 deg) remains fairly legible, but, as may be anticipated, visibility decreases with increased eccentricity from the center. However, the degradation of image visibility with the eccentricity illustrated in this image is much lower than the degradation simulated by Yeshurun and Schwartz,[36] who used the cortical area as the variable controlling the simulation. Our simulations represent only the loss of undetected contrast. It is possible that text recognition requires more than just detection; e.g., it may require discrimination of the orientation of features. Nevertheless, even when the simulations are repeated with steeper degradation obtained for orientation discrimination thresholds, they are still substantially less degraded than those presented by Yeshurun and Schwartz.

DISCUSSION

Spatial inhomogeneities are an important feature of the visual system's organization. Nonuniform processing starts with the spatially variable sampling rate of the photoreceptors, featuring a high density centrally and a gradually decreasing density toward the retinal periphery. The nonuniform organization continues throughout the system up to the retinotopic mapping of the visual field onto the surface of the striate cortex.[37] This nonuniform structure commonly is considered a biologically necessary, visually unfavorable characteristic of the visual system and is assumed to be a response to limitations of the nonuniform imaging by the eye's optics or as a method for reduction of data rate in response to limited processing capabilities.[38] Schwartz[37] suggested that the anatomic organization of the cortex as a complex logarithmic mapping of the retinal surface may be useful in providing the visual system with its size-invariance capability. However, such size invariance would apply only in the periphery, while the same transform would be size variant near the fovea.[29] As was pointed out by Cavanagh,[40] however, there is no evidence of such deficiencies of size invariance for the fovea. In any case, the size-scaling property of the complex logarithm (global or local) is applicable only to suprathreshold information. We are analyzing the invariant visibility of near-threshold features with size–distance changes. Such invariance is a prerequisite for the size invariance suggested by Schwartz[39] and Cavanagh.[40]

The excellent fit of the results presented here suggests that the model that we propose adequately represents the behavior of the visual system. The model presented here accounts only for suboptimal invariance. The limitation on the invariance is equal at any eccentricity to the limitation on the invariance of contrast sensitivity with changes in distance at the center of the fovea. However, for the 4-octave range of frequencies straddling the peak of the CSF (1–16 cycles/deg), the deviation from optimal invariance is small. This deviation is even smaller if the CSF is measured by using wide-band (1 octave) Gabor-patches stimuli. We believe that such CSF's are more relevant to the interpretation of form vision.[24]

Careful examination of the data and the fits presented here reveals that for large eccentricities and low spatial frequencies the data points tend to fall above the line fitted by the model. These deviations from the model at large eccentricities are more apparent for orientation identification data than for any of the contrast detection data. Such deviations may represent changes in peripheral vision that cannot be accounted for by simple loss of contrast sensitivity but may involve loss of phrase relationships.[41] The deviations may also be the result of aliasing of high frequencies in the periphery, which can prevent orientation discrimination while detection is maintained.

Our model's size-invariant condition for the threshold

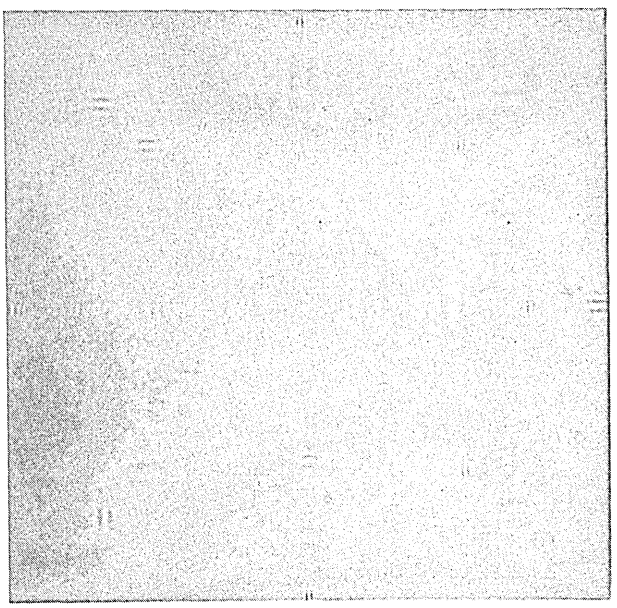

Fig. 8. Equal-visibility chart, including variations in both size and contrast. When fixation is maintained at the center, all patches should be of equal visibility (the contrast is three times the threshold contrast). In this chart, for any eccentricity we may trade size for contrast and maintain visibility. The threshold chart corresponding to Anstis's[46] letter chart cannot be reproduced in print because of the low contrasts. This image was generated under the assumption that the full frame spans 32 deg of visual angle. However, the effect should be largely distance invariant. The orientation discrimination data (subject JY) were used. Thus the discrimination of patch orientation should be equal for all eccentricities and sizes presented on the chart.

case is identical to the exact relationship found by Carlson *et al.*[11] and Braccini[42] for linear systems. The difference between a nonlinear threshold system and a linear system and the explicit distinction between contrast and image amplitudes as the inputs to the system distinguish our work from the previous analyses. Direct consideration of the threshold requirements also enables us to notice the suboptimal nature of the invariance at threshold that was missed by Klopfenstein and Carlson[12] because they considered only the normalized sensitivity. The bilinear form of the eccentricity and spatial frequency variables in the normalized expression alone is not sufficient for the threshold invariance.

Robson and Graham[18] found that, if the contrast detection threshold is plotted as a function of eccentricity (expressed in pattern periods rather than degrees), the data could be fitted by straight lines with the same slope for all spatial frequencies. It easily can be seen that their number-of-periods rule of thumb is equivalent to our requirement that the slopes have the same ratios as the corresponding spatial frequencies. Pointer and Hess[17] have replicated the same results for both the horizontal and the vertical meridian and recently showed that the same relationship also holds along the oblique meridian of the retina.[43] Thus the relationship required by our model is satisfied along the horizontal, vertical, and oblique meridians of the retina, despite the large absolute differences in sensitivity and in the value of the eccentricity constant among the meridian (Table 1). Existence of these relations along each meridian separately is necessary only to maintain invariance.[12]

Comparison of results from different studies of peripheral function is usually difficult. Johnson *et al.*,[44] comparing detection and resolution properties of visual function as a function of eccentricity, used standardized conditions and measured the same dependent variable (threshold luminance) for both tasks. They compared the detection of circular targets with the discrimination of circular targets from square targets and used the same observers for all tests. Our method of fitting the data with the postulated, underlying model enabled us to compare the results of other studies of grating detection with the results of our study of discrimination of grating orientation. Like Johnson *et al.*[44] and Fleck,[13] we determined that the discrimination sensitivity gradient is steeper than the detection sensitivity profile.

Thomas[20] found individual variations in the effect of eccentricity on the identification/detection performance ratio (*I/D*). However, his composite data do show a decrease of *I/D* when intermediate and high frequencies are used. Such decreases are consistent with a steeper gradient of identification than that of detection. Thomas offered two possible interpretations of the results: That the bandwidths of higher-frequency mechanisms increase with eccentricity or that for higher frequencies only one mechanism responds to each of the two stimuli, thus permitting detection but not discrimination.

Since we expressed the difference quantitatively by means of the calculated eccentricity constant, we also were able to compare the studies with regard to the steepness of the drop in sensitivity with eccentricity along different meridia and the relationships between detection thresholds for chromatic and luminance gratings.

Garcia-Perez[45] and Fleck[13] proposed models that incorporate visual inhomogeneity, based on multiple, spatially limited channels centered in the fovea. Their models were suggested as useful tools for analysis of various visual perceptual phenomena that may arise from nonuniform processing, such as the Gestalt frame-of-reference effect.[45] However, the role of the nonuniform visual system in aiding size–distance invariance was not considered. The spatial extent of various frequency channels was determined by using sinusoidal gratings. In these models for each spatial frequency there is only one threshold, limiting all features of that frequency to a fixed radius around the fovea. In our model higher-contrast features will be visible farther into the periphery than lower-contrast features of the same spatial frequency.

Our model provides a new, more powerful tool for analyzing the visibility of displays, generating equal-visibility displays, or generating displays of predesigned variable visibility. It can be considered an analytical extension of the equal-visibility acuity chart presented by Anstis.[46] This extension is achieved by adding the dimension of contrast (Fig. 8) and by providing a general analysis that is not limited to acuity letters only. Our analysis and data could be used to predict Anstis's[46] results if we assume that letter recognition requires discrimination of the orientation of features at some critical frequency expressed in cycles/letter. Using the average eccentricity constant from our two subjects, we can see that for any fixed, normalized threshold the size of the letter than can

be discriminated as a function of f (where f is the fundamental frequency of the letter) should vary linearly with the angle of eccentricity as 0.05θ, where θ is the eccentricity. Anstis[46] found in his experiment for high-contrast letters that the size of the discriminated letter varied with the eccentricity as 0.046θ. This excellent agreement suggests that orientation discrimination rather than contrast detection ($a = 0.03$) is required for letter identification.

ACKNOWLEDGMENTS

This research was supported in part by National Institutes of Health grant EY05957 and by a grant from the Teubert Charitable Trust Foundation. We thank George Young for valuable technical help and Steve Lubars for programming help. This research was presented in part at the annual meeting of the Association for Research in Vision and Ophthalmology, May 1990, Sarasota, Florida.

E. Peli is also with the Department of Ophthalmology of the Harvard Medical School and of the Tufts University School of Medicine, Boston, Massachusetts.

R. B. Goldstein is also with the Department of Ophthalmology, Harvard Medical School, Boston, Massachusetts.

REFERENCES AND NOTES

1. N. S. Sutherland, "Outlines of a theory of visual pattern recognition in animal and man," Proc. R. Soc. London Ser. B **171,** 297–317 (1968).
2. A. P. Ginsburg, "Visual information processing based on spatial filters constrained by biological data," Ph.D. dissertation (Cambridge University, Cambridge, 1978).
3. A. Fiorentini, L. Maffei, and G. Sandini, "The role of high spatial frequencies in face perception," Perception **12,** 195–201 (1983).
4. D. H. Parish and G. Sperling, "Object spatial frequencies, retinal spatial frequencies and the efficiency of letter discrimination," Vision Res. **31,** 1399–1415 (1991).
5. T. Hayes, M. C. Morrone, and D. C. Burr, "Recognition of positive and negative bandpass-filtered images," Perception **15,** 595–602 (1986).
6. J. Norman and S. Ehrlich, "Spatial frequency filtering and target identification," Vision Res. **27,** 87–96 (1987).
7. M. A. Georgeson and G. D. Sullivan, "Contrast constancy: deblurring in human vision by spatial frequency channels," J. Physiol. **252,** 627–656 (1975).
8. J. J. Kulikowski, "Effective contrast constancy and linearity of contrast sensation," Vision Res. **16,** 1419–1431 (1976).
9. R. F. Hess, A. N. Bradley, and L. Piotrowski, "Contrast coding in amblyopia. I. Differences in the neural basis of human amblyopia," Proc. R. Soc. London **127,** 309–330 (1983).
10. B. R. Stephens and M. S. Banks, "The development of contrast constancy," J. Exp. Child Psychol. **40,** 528–547 (1985).
11. C. R. Carlson, R. W. Klopfenstein, and C. H. Anderson, "Spatially inhomogeneous scaled transforms for vision and pattern recognition," Opt. Lett. **6,** 386–388 (1981).
12. R. W. Klopfenstein and C. R. Carlson, "Theory of shape-invariant imaging system," J. Opt. Soc. Am. A **1,** 1040–1053 (1984).
13. H. J. Fleck, "Measurement and modeling of peripheral detection and discrimination thresholds," Biol. Cybern. **61,** 437–446 (1989).
14. K. T. Mullen, "Color vision as a post receptoral specialization of the central visual field," Vision Res. **31,** 119–130 (1991).
15. A 5-cycle/deg feature refers to a localized image feature with a spatial spectral mean frequency of 5 cycles/deg, such as a Gabor patch or any other localized luminance patch. Although real image features may have higher frequencies, the contrast at those frequencies will generally be much lower and thus will be subthreshold and inconsequential for our discussion.
16. M. S. Banks, W. S. Geisler, and P. J. Bennett, "The physical limits of grating visibility," Vision Res. **27,** 1915–1924 (1987).
17. J. S. Pointer and R. F. Hess, "The contrast sensitivity gradient across the human visual field: with emphasis on the low spatial frequency range," Vision Res. **29,** 1133–1151 (1989).
18. J. G. Robson and N. Graham, "Probability summation and regional variation in contrast sensitivity across the visual field," Vision Res. **21,** 409–418 (1981).
19. M. W. Cannon, Jr., "Perceived contrast in the fovea and periphery," J. Opt. Soc. Am. A **2,** 1760–1768 (1985).
20. J. P. Thomas, "Effect of eccentricity on the relationship between detection and identification," J. Opt. Soc. Am. A **4,** 1599–1605 (1987).
21. A. M. Derrington and G. B. Henning, "Pattern discrimination with flickering stimuli," Vision Res. **21,** 597–602 (1981).
22. J. P. Thomas, "Detection and identification: how are they related?" J. Opt. Soc. Am. A **2,** 1457–1467 (1985).
23. H. Strasburger, L. O. Harvey, Jr., and I. Rentschler, "Contrast threshold for identification of numeric characters in direct and eccentric view." Percept. Psychophys. (to be published).
24. E. Peli, R. B. Goldstein, G. M. Young, and L. E. Arend, "Contrast sensitivity functions for analysis and simulation of visual perception," in *Noninvasive Assessment of the Visual System,* Vol. 3 of 1990 OSA Technical Digest Series (Optical Society of America, Washington, D.C., 1990), pp. 126–129.
25. H. R. Lieberman and A. P. Pentland, "Microcomputer-based estimation of psychophysical thresholds: the best PEST," Behav. Res. Methods Instrum. **14,** 21–25 (1982).
26. R. Hilz and C. R. Cavonius, "Functional organization of the peripheral retina: sensitivity to periodic stimuli," Vision Res. **14,** 1333–1337 (1974).
27. J. P. Rijsdijk, J. N. Kroon, and G. J. van der Wildt, "Contrast sensitivity as a function of position on the retina," Vision Res. **20,** 235–241 (1980).
28. D. Regan and K. I. Beverley, "Visual fields described by contrast sensitivity, by acuity, and by relative sensitivity to different orientations." Invest. Ophthalmol. Vis. Sci. **24,** 754–759 (1983).
29. G. T. Timberlake, E. Peli, and R. A. Augliere, "Visual acuity measurement with a second-generation scanning laser ophthalmoscope," in *Noninvasive Assessment of the Visual System,* Vol. 4 of 1987 Technical Digest Series (Optical Society of America, Washington, D.C., 1987), pp. 4–7.
30. J. M. Woodhouse and H. B. Barlow, "Spatial and temporal resolution and analysis," in *The Senses,* H. B. Barlow and J. D. Mollon, eds. (Cambridge U. Press, Cambridge, 1982), Chap. 8, pp. 133–164.
31. M. D. Wilkinson, L. N. Thibos, and M. W. Cannon, "Contrast constancy: neural compensation for image attenuation," Invest. Ophthalmol. Vis. Sci. Suppl. **31,** 323 (1990).
32. A. P. Ginsburg, "Is the illusory triangle physical or imaginary?" Nature (London) **257,** 291–220 (1975).
33. C. W. Tyler, "Is the illusory triangle physical or imaginary?" Perception **6,** 603–604 (1977).
34. E. Peli, "Contrast in complex images," J. Opt. Soc. Am. A **7,** 2032–2040 (1990).
35. G. T. Timberlake, E. Peli, E. A. Essock, and R. A. Augliere, "Reading with macular scotoma. II. Retinal locus for scanning text," Invest. Ophthalmol. Vis. Sci. **28,** 1268–1274 (1987).
36. Y. Yeshurun and E. L. Schwartz, "Shape description with a space-variant sensor: algorithms for scan-path, fusion, and convergence over multiple scans," IEEE Trans. Pattern Anal. Mach. Intell. **11,** 1217–1222 (1989).
37. E. L. Schwartz, "Spatial mapping in the primate sensory projection: analytic structure and relevance to perception," Biol. Cybern. **25,** 181–194 (1977).
38. Y. Y. Zeevi, N. Peterfreund, and E. Shlomot, "Pyramidal image representation in nonuniform systems," in *Visual Communications and Image Processing '88,* T. R. Hsing, ed., Proc. Soc. Photo-Opt. Instrum. Eng. **1001,** 563–571 (1988).
39. E. L. Schwartz, "Cortical anatomy, size invariance, and spatial frequency analysis," Perception **10,** 455–468 (1981).
40. P. Cavanagh, "Size invariance: reply to Schwartz," Perception **10,** 469–474 (1981).

41. I. Rentschler and B. Trentwein, "Loss of spatial phase relationships in extrafoveal vision," Nature (London) **313,** 308–310 (1985).
42. C. Braccini, "Scale-invariant image processing by means of scaled transforms or form-invariant, linear shift-variant filters," Opt. Lett. **8,** 392–394 (1983).
43. J. S. Pointer and R. F. Hess, "The contrast sensitivity gradient across the major oblique meridians of the human visual field," Vision Res. **30,** 497–501 (1990).
44. C. A. Johnson, J. L. Keltner, and F. Balestery, "Effects of target size and eccentricity on visual detection and resolution," Vision Res. **18,** 1217–1222 (1978).
45. M. A. Garcia-Perez, "Space-variant visual processing: spatially limited visual channels," Spatial Vision **3,** 129–142 (1988).
46. S. N. Anstis, "A chart demonstrating variations in acuity with retinal position," Vision Res. **14,** 589–592 (1974).